Volume 12 | Number 32 | 28 August 2014 | Pages 6017–6280

Organic & Biomolecular Chemistry

www.rsc.org/obc

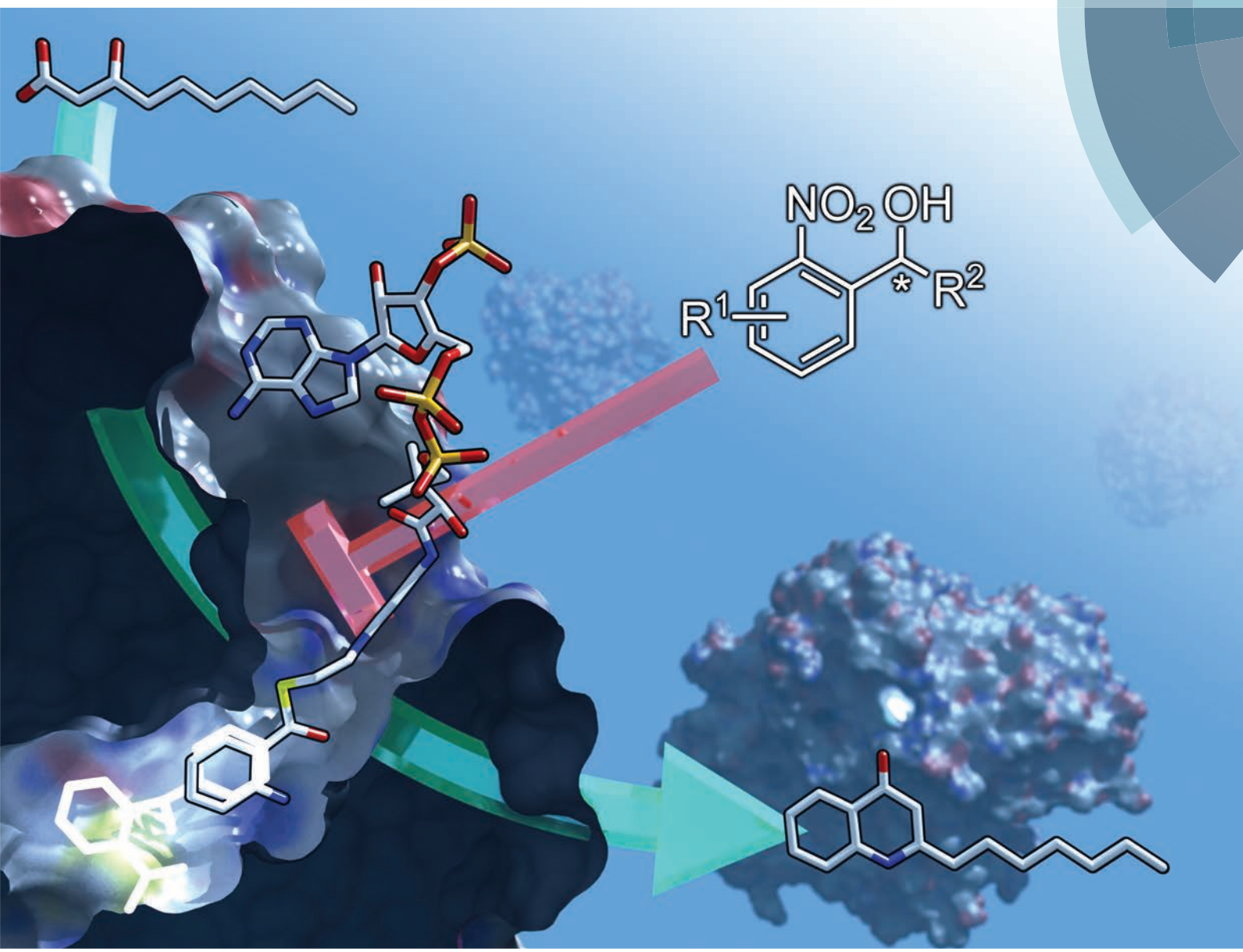

ISSN 1477-0520

ROYAL SOCIETY OF CHEMISTRY

PAPER

Martin Empting, Rolf W. Hartmann *et al.*

From *in vitro* to *in cellulo*: structure–activity relationship of (2-nitrophenyl)-methanol derivatives as inhibitors of PqsD in *Pseudomonas aeruginosa*

Organic & Biomolecular Chemistry

PAPER

View Article Online
View Journal | View Issue

Cite this: *Org. Biomol. Chem.*, 2014, **12**, 6094

From *in vitro* to *in cellulo*: structure–activity relationship of (2-nitrophenyl)methanol derivatives as inhibitors of PqsD in *Pseudomonas aeruginosa*†

Michael P. Storz,[a] Giuseppe Allegretta,[a] Benjamin Kirsch,[a] Martin Empting*[a] and Rolf W. Hartmann*[a,b]

Received 3rd April 2014,
Accepted 29th May 2014

DOI: 10.1039/c4ob00707g

www.rsc.org/obc

Recent studies have shown that compounds based on a (2-nitrophenyl)methanol scaffold are promising inhibitors of PqsD, a key enzyme of signal molecule biosynthesis in the cell-to-cell communication of *Pseudomonas aeruginosa*. The most promising molecule displayed anti-biofilm activity and a tight-binding mode of action. Herein, we report on the convenient synthesis and biochemical evaluation of a comprehensive series of (2-nitrophenyl)methanol derivatives. The *in vitro* potency of these inhibitors against recombinant PqsD as well as the effect of selected compounds on the production of the signal molecules HHQ and PQS in *P. aeruginosa* were examined. The gathered data allowed the establishment of a structure–activity relationship, which was used to design fluorescent inhibitors, and finally, led to the discovery of (2-nitrophenyl)methanol derivatives with improved *in cellulo* efficacy providing new perspectives towards the application of PqsD inhibitors as anti-infectives.

Introduction

Until recently, bacterial communities were seen as nothing more than an accumulation of autonomous single-celled organisms. But today, we are aware that bacteria use cell-to-cell communication systems like *quorum sensing* (QS) to behave collectively rather than as individuals.[1] Small diffusible molecules are produced by single bacterial cells that can be released into the environment and detected by surrounding bacteria. Upon proliferation, the extracellular signal molecule concentrations increase along with cell density. Once a certain threshold is reached, receptors are activated by these autoinducers resulting in population-wide changes in gene expression. This concerted switch from low- to high-cell-density mode allows single bacterial cells to limit their group-beneficial efforts to those cell densities which guarantee an effective group outcome. Even if QS may not be directly essential for the survival of a singular bacterial cell, it is very important for bacteria–host interactions and pathogenesis upon bacterial infections in general. In this regard, QS regulates a variety of virulence factors, which contribute to breaking the first line defences and damaging surrounding tissues leading to dissemination, systemic inflammatory-response syndrome, multiple organ failure, and, finally, death of the host.[2] Furthermore, QS contributes to the collective coordination of biofilm formation, a key reason for bacterial resistance against conventional antibiotics in clinical use.[3] Thus, the importance of these regulatory systems could be exploited for the design of novel anti-infectives.

Several groups have successfully targeted QS, which is discussed as an alternative to the traditional treatment using bactericidal or bacteriostatic agents (for reviews see ref. 4 and 5). Novel anti-virulence compounds ideally decrease pathogenicity without affecting bacterial survival or growth, whereas it is believed that no or less selection pressure is posed on the bacteria. Hence, a reduced rate of newly occurring resistances, which gradually render existing antibiotics ineffective, is expected.[6]

Among bacteria, very different communication systems based on distinct autoinducers are utilized. Gram-positive bacteria primarily use modified oligopeptides, whereas *N*-acyl homoserine lactones are a major class of signal molecules in Gram-negative bacteria.[1] The opportunistic pathogen *P. aeruginosa* additionally utilizes a characteristic *pqs* system, which is based on the quinolone PQS (*Pseudomonas* Quinolone Signal) and its biosynthetic precursor HHQ (2-heptyl-4-quinolone) (Fig. 1).[7]

[a]*Helmholtz-Institute for Pharmaceutical Research Saarland (HIPS), Campus C23, 66123 Saarbrücken, Germany. E-mail: rolf.hartmann@helmholtz-hzi.de; Fax: +49 681 302 70308; Tel: +49 681 302 70300*

[b]*Pharmaceutical and Medicinal Chemistry, Saarland University, Campus C23, 66123 Saarbrücken, Germany*

†Electronic supplementary information (ESI) available: Synthesis and analytics of all synthetic intermediates and all substrates used in the enzyme inhibition assay as well as procedure of the mutagenicity test; HHQ and PQS inhibition in the PA14 wild-type strain. See DOI: 10.1039/c4ob00707g

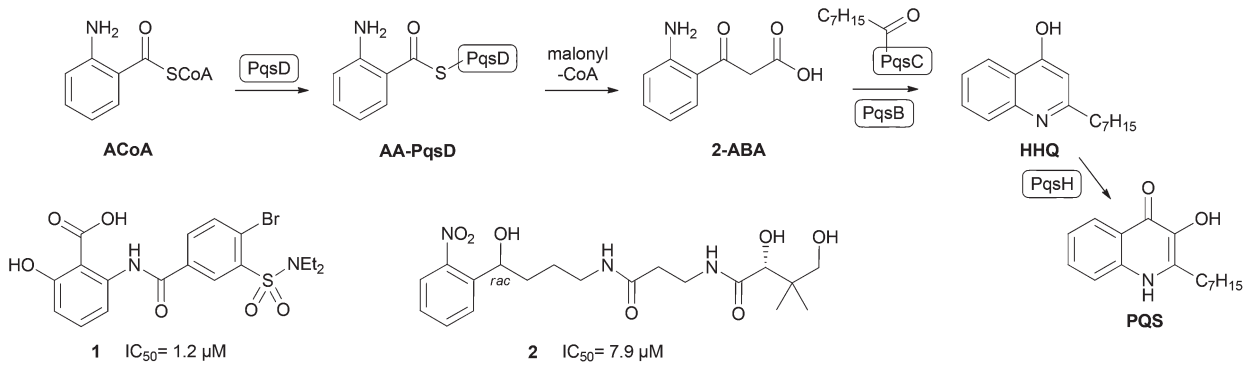

Fig. 1 Role of PqsD in HHQ and PQS biosynthesis (top). Structures of previously reported PqsD inhibitors **1** and **2**.

Both are able to activate the transcriptional regulator PqsR leading to the production of various virulence factors like pyocyanin and hydrogen cyanide (HCN).[8] We have shown, that PqsR antagonists efficiently decrease pyocyanin production and pathogenicity of *P. aeruginosa* PA14.[9,10] Furthermore, HHQ and PQS contribute to the formation of biofilms.[3]

Biosynthesis of HHQ and PQS is accomplished by proteins encoded by the *pqsABCD* operon. Thereby, experiments using transposon knockout mutants identified PqsD as key enzyme in the cellular signal molecule production route.[11,12] Recently, Dulcey *et al.* reported that cytoplasmic PqsD catalyses the condensation of anthraniloyl-CoA (ACoA) and malonyl-CoA to 2-aminobenzoylacetate (2-ABA, Fig. 1).[13] The resulting reactive intermediate is then processed to HHQ by PqsC using octanoic acid as substrate. This second reaction step is supported by PqsB by an unknown mechanism. Interestingly, PqsD alone is also capable of generating HHQ *in vitro* directly from ACoA using β-ketodecanoic acid as secondary substrate.[14] This enzymatic reaction has been routinely exploited by us to evaluate PqsD inhibitors.[14–18] Inhibition of PqsD is an attractive strategy to interfere with QS-controlled infection mechanisms, since it is essential for cellular HHQ/PQS formation. A *pqsD* transposon mutant strain of *P. aeruginosa* PAO1, which is deficient in PQS formation, shows decreased levels of pyocyanin and HCN as well as reduced lethality in nematodes.[11] Furthermore, putative inhibitors of PqsA, an enzyme involved in earlier stages of HHQ biosynthesis, block the cellular production of the corresponding signal molecules, prevent systemic dissemination, and attenuate mortality in infected mice.[19]

Derived from compounds active against FabH, a structurally and functionally related enzyme, we have identified and optimized the first PqsD inhibitors demonstrating IC_{50} values in the single-digit micromolar range (Fig. 1, **1**).[14,15] Unfortunately, these compounds had no pronounced effect on the extracellular signal molecule levels in cell-based assays using *P. aeruginosa* PA14 (unpublished data). Recently, in a ligand-based approach we have identified compound **2** as a novel inhibitor of PqsD (Fig. 1).[16] Ligand efficiency-guided optimisation led to compound **3** (Fig. 2), which was used for an initial examination of the effects on PA14 cells mediated by

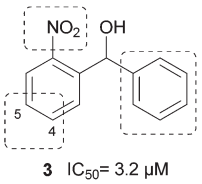

Fig. 2 Systematically varied structural features of inhibitor **3**.

PqsD inhibition.[16] Indeed, this compound was capable of reducing the HHQ and PQS levels. Furthermore, biofilm formation was significantly inhibited and no antibiotic effects were observed.

Binding studies of **3** revealed apparent irreversibility and that binding occurs near the active site residues.[17] Both enantiomers showed similar affinity but contrary thermodynamic profiles. Based on site-directed mutagenesis, isothermal titration calorimetry (ITC) analysis, and molecular docking, explicit binding modes were proposed. In these predicted enzyme–inhibitor complexes both enantiomers reside in nearly identical positions with the main difference being the orientation of the hydroxyl group at the stereogenic center.[17]

Herein, we present a target-oriented (*in vitro*) structure–activity relationship and optimization of this compound class based on the (2-nitrophenyl)methanol scaffold by systematic structure variation (Fig. 2) investigating also the time-dependent onset of inhibition. Previously, we reported, that a tetrahedral geometry including an acceptor function is favoured for the linker between both phenyl rings.[16] However, the intrinsic nitrophenyl moiety bears an increased risk of toxic, mutagenic and carcinogenic side effects.[20] Thus, we evaluated the mutagenicity in Ames *Salmonella* assays and investigated suitable chemical replacements. Additionally, the influences of substituents with opposed electronic and hydrophilic properties in 4- and 5-position of the nitrophenyl moiety were studied. Furthermore, a variety of aliphatic and aromatic residues instead of the second phenyl ring were examined.

The gathered information enabled us to design fluorescent inhibitors, which may be useful tools to investigate enzyme inhibitor interactions and to visualize the target in cells.[21,22]

Finally, selected compounds were examined regarding their potency to inhibit signal molecule production in *P. aeruginosa* PA14 cells. Thereby, we additionally applied a novel strategy to reduce costs and time by the usage of a *pqsH*-deficient mutant which has been selected from a transposon mutant library.[23] This procedure allows to evaluate the potency of a compound solely by quantification of HHQ instead of two signal molecules. In this way we identified compounds with increased *in cellulo* activity while a low molecular weight is retained (<250 Da). These optimized fragment-like molecules provide the potential for further improvements by a fragment growing approach. Additionally, an attempt to correlate *in vitro* data with the effects observed in the cellular assays is made.

Results and discussion

Chemistry

In order to find alternatives to the nitro group, a variety of molecules with different chemical functionalities were synthesized (Scheme 1). Assembly of (2-aminophenyl)(phenyl)-methanol **8** started with the formation of Boc-protected aniline **5**. Ortho-lithiation by *tert*-butyllithium and subsequent reaction with benzaldehyde yielded the alcohol **6**. The desired product **8** was obtained by a two-step deprotection using trifluoroacetic acid and basic hydrolysis. This route also provided access to the cyclic carbamate **7**.

The carboxylate **11** was prepared by iso-propylmagnesium chloride-mediated iodine–magnesium exchange on methyl 2-iodobenzoate **9** and subsequent addition to benzaldehyde. This reaction is followed by spontaneous cyclisation yielding lactone **10**, which was hydrolyzed under basic conditions to yield the desired carboxylate. An analogous method employing iodine–magnesium exchange was used for synthesis of the trifluoromethyl and nitril derivatives **14** and **15**. In the case of compounds **21–25** and **28–29**, corresponding aldehyde precursors were commercially available. Hence, the desired products were prepared by direct addition of phenylmagnesium chloride.

The synthesis of (2-nitrophenyl)methanol derivatives **3**, **33–35**, **39**, **40**, **43–44**, and **47–86** followed the general pathways outlined in Scheme 2. For all compounds, in which Z^1 or Z^2 were exclusively substituted by hydrogen or methyl, phenylmagnesium chloride was added to **36–38** to accomplish iodine–magnesium exchange in *ortho* position to NO_2 as described by Knochel and coworkers.[24] The generated Grignard reagents were reacted with the appropriate aldehydes to form the desired products.

For synthesis of the methoxy derivatives **43** (Z^1 = OMe) and **44** (Z^2 = OMe) from **41** and **42** we utilized 4-methoxyphenylmagnesium bromide as novel reagent to accomplish

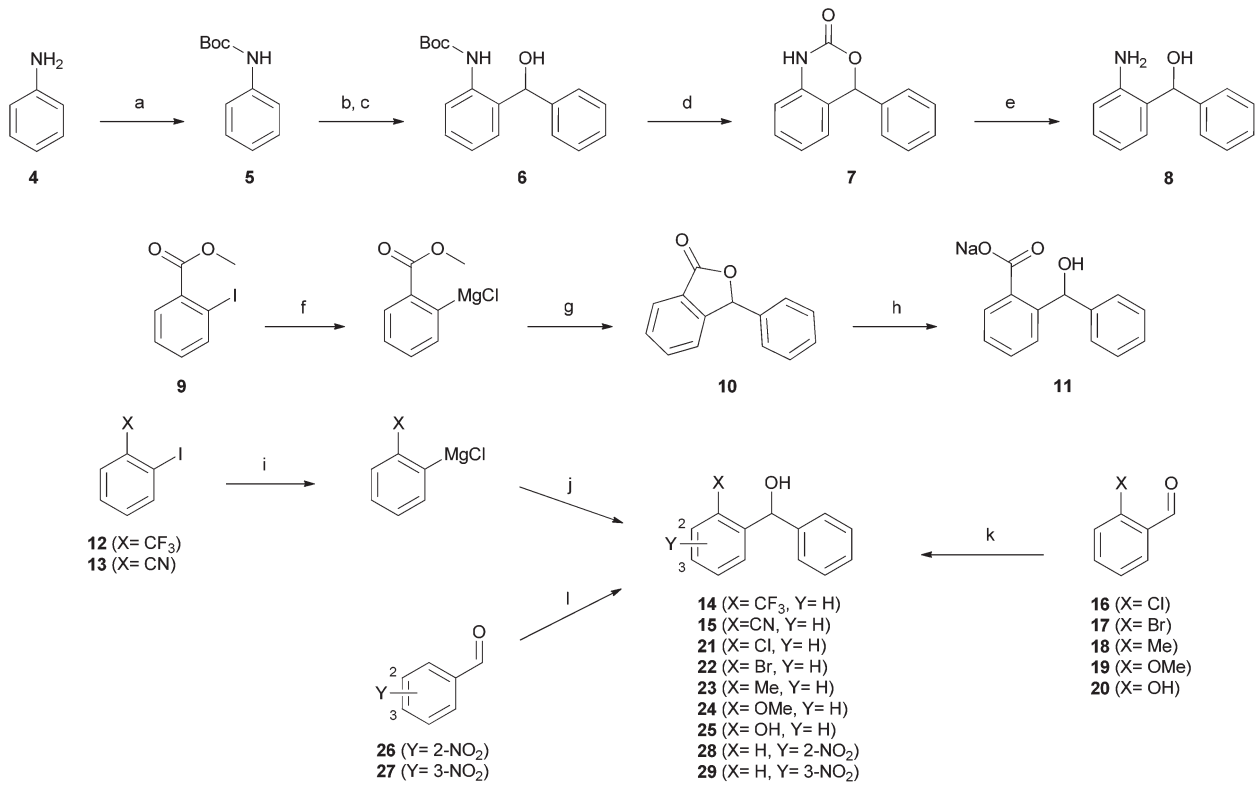

Scheme 1 Synthesis of compounds **8**, **11**, **14–15**, **21–25**, and **28–29**. Reagents and conditions: (a) Boc_2O, THF, reflux, 38%; (b) *t*BuLi, THF, −60 °C; (c) benzaldehyde, THF, −20 °C, 35% (2 steps); (d) TFA, DCM, 0 °C–room temp, 78%; (e) KOH, MeOH–H_2O, reflux, 17%; (f) iPrMgCl, THF, −40 °C; (g) benzaldehyde, THF, −40 °C, 63% (2 steps); (h) NaOH, MeOH–H_2O, 50 °C, 39%; (i) iPrMgCl, THF, −40 °C; (j) benzaldehyde, THF, −40 °C, 47–71% (2 steps); (k) PhMgCl, THF, 0–50 °C, 36–92%; (l) PhMgCl, THF, −40 °C, 7–12%.

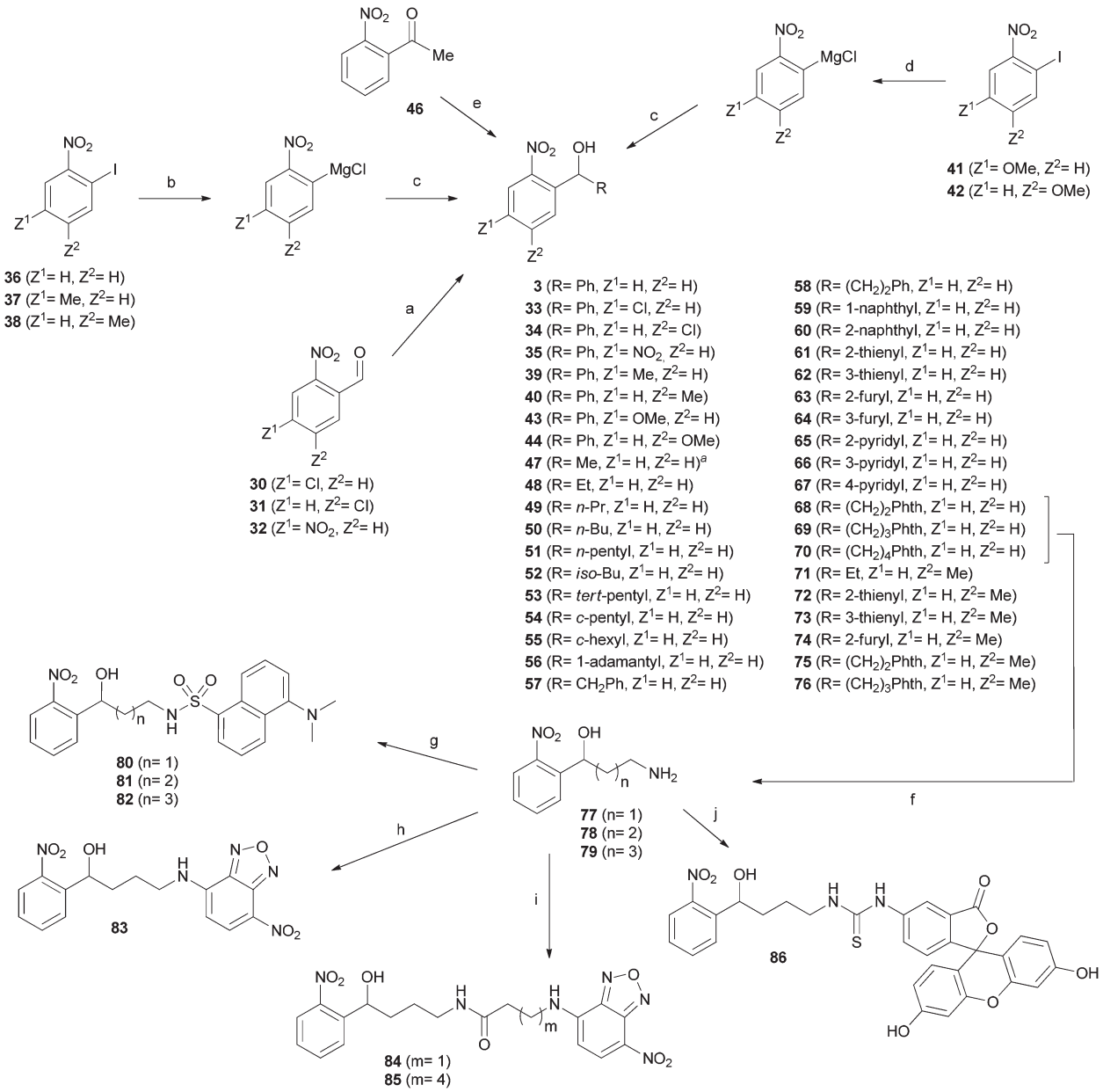

Scheme 2 Synthesis of compounds **3**, **33–35**, **39–40** and **43–44** and **47–86**. Reagents and conditions: (a) PhMgCl, THF, −40 °C; 20–58%; (b) PhMgCl, THF, −40 °C; (c) aldehyde, THF, −40 °C, 11–86% (2 steps); (d) 4-methoxyphenylmagnesium bromide, THF, −40 °C; (e) $NaBH_4$, MeOH, 0 °C–room temp, 62%; (f) hydrazine hydrate, EtOH, reflux, 62–89%; (g) NBD chloride, $NaHCO_3$, MeOH, room temp – 50 °C, 40%; (h) HOOC-$(CH_2)_m$NH-NBD (**84i**, **85i**), EDC·HCl, HOBt·H_2O, NMM, acetonitrile, room temp, 32–46%; (i) dansyl chloride, TEA, DCM, room temp, 29–45%; (j) fluorescein iso-thiocyanate, DIEA, DMF, room temp, 36%.

iodine–magnesium exchange in *ortho*-iodo-nitrobenzenes. Application of this method to a broader range of substrates will be discussed elsewhere.

Fluorescent derivatives were prepared by cleavage of the phthalimide moiety of **68–70** *via* the Ing-Manske procedure. The released amines **77–79** served as a starting point for the introduction of fluorophores. Coupling these amines with dansyl chloride yielded derivatives **80–82**. Direct attachment of NBD to the amine **78** using NBD-chloride afforded **83**, whereas **84** and **85** were synthesized by coupling with the NBD containing carboxylic acids. The fluorescein derivative **86** was formed upon reaction with fluorescein iso-thiocyanate.

Essentiality of the nitro-group and Ames test

After synthesis, compounds were evaluated regarding their inhibitory activity against heterologously expressed and purified PqsD using ACoA and β-ketodecanoic acid as substrates.[14] Until recently, β-ketodecanoic acid instead of malonyl-CoA has been considered as the second substrate in HHQ synthesis, since it has been shown, that addition of β-ketodecanoic acid

to the anthraniloyl-PqsD complex leads to HHQ formation *in vitro*.[14] We have clearly shown that (2-nitrophenyl)methanol derivatives interfere with the formation of the anthraniloyl-PqsD complex itself, which allows further usage of β-ketodecanoic acid independently of its function in the bacterial cells.[17]

First, a variety of substituents replacing the nitro group in *ortho* position were tested. An amino group (**8**) in analogy to ACoA, which served as template for the inhibitor design,[16] led to an inactive compound. This was also true for substituents with electron-withdrawing properties similar to the nitro group, as trifluoromethyl (**14**), nitril (**15**) and halogens (**21**, **22**). Furthermore, no activity was observed for molecules bearing potential hydrogen bond acceptors like **7**, **10**, the carboxylate **11**, **24** and **25**. Since the nitro group seems to be essential for activity, we shifted the position in *meta* or *para* position (**28**, **29**), but inhibitory potency was again completely abolished. An initial toxicity study provided promising results, since no toxic effect against human THP-1 macrophages was observed at 250 μM of compound **3**.[16] To assess the mutagenic risk of the compound class, Ames *Salmonella* assays were performed. Compound **3** was tested on *Salmonella typhimurium* derived strains TA100, TA1535 and TA102 with and without metabolic activation by liver homogenate (S9 mix). No biologically relevant increase in the number of revertant colonies was observed at dose levels up to 5000 μg per plate. Thus, the nitro group was retained and we focused our efforts on the improvement of inhibitory activity by introduction of additional substituents into the nitrophenyl moiety.

In vitro SAR

Recently, we have reported extensive studies on the mode of action of the (2-nitrophenyl)methanol scaffold.[17] In this regard, we demonstrated a time-dependent onset of inhibition based on a slow non-covalent (reversible) interaction. As we have observed that inhibition onset levels out after 20 min of preincubation for compound **3**,[17] we consider a period of 30 min appropriate for the rapid evaluation of the set of novel compounds ($n \sim 50$) described herein. Additionally, we measured the inhibitory activity using only 10 min of preincubation to gain qualitative insight into the effect of inhibitor modifications on binding behaviour.

This examination is relevant, as it has been reported that time-dependency of enzyme–inhibitor interactions can have significant impact in the efficacy of compounds in the cellular system.[25]

First, we re-evaluated our starting compound **3** applying an optimized protocol for the prolonged pre-treatment period of enzyme with inhibitor (Table 1). As described earlier,[17] an improvement of potency was observed rendering this compound now a sub-micromolar PqsD inhibitor.

In a subsequent step, we investigated the effect of different substituents within the nitrophenyl moiety. Compounds bearing electron-withdrawing substituents (EWG) as chlorine (**33**, **34**) or nitro (**35**) showed diminished inhibitory activity (Table 1). However, concerning target affinity (IC_{50} at 30 min of preincubation) the *para* substitution pattern (Z^2 in Table 1) seems to be more favourable. In contrast, introduction of the electron-donating (EDG) methyl (**39**, **40**) or methoxy (**43**, **44**) groups led to potent compounds with IC_{50} values in the range of the unsubstituted **3**. Again, a preference for the introduction of substituents at Z^2 was observed (**40**, **44**). These observations are in accordance with our proposed binding mode reported earlier,[17] as the *para* position to the nitro group provides more space to accommodate additional substituents. An explanation for the general detrimental effect of EWGs on affinity could be that the nitro group functions as hydrogen bond acceptor (as in our proposed binding model). This ability might possibly be diminished by electron-withdrawing substituents. Unfortunately, none of the modifications installed in this part of the scaffold led to an improvement of inhibitor potency. However, comparing the determined IC_{50} for 10 min and 30 min, it seems that the Z^2 position provides the opportunity to modulate the binding behaviour. Through the choice of either methyl (EDG) or chloro (EWG) substituents, the onset (see IC_{50} at 10 min) can be either slightly accelerated (**3** *vs.* **40**) or slowed down (**3** *vs.* **34**).

In light of the results gathered so far, we kept the unsubstituted nitrophenyl moiety constant and turned our attention to the second residue R of the methanol moiety. Hydrogen or linear alkyl chains of different length were introduced (**45**, **47–51**). Thereby, shorter residues up to ethyl (**45**, **47**, and **48**) were favoured over longer variants (**49–51**). A plausible explanation is the increasing entropic penalty caused by the limitation of rotational freedom upon formation of the inhibitor–enyzme complex.

Except iso-butyl-bearing compound **52**, branched and cyclic isomers **53–56** generally inhibited PqsD less efficiently than their linear congeners. This might be due to the narrow entrance channel, which hampers the binding of the bulky residues.

Short alkyl linkers were inserted between the tetrahedral carbon and the phenyl group, but neither compound **57** nor **58** showed improved IC_{50} values compared to **3**. Thus, we concluded that direct attachment to the methanol moiety brings the aromatic residue in an optimal position and fused a second benzene ring. But the resulting 1-naphthyl and 2-naphthyl isomers **59** and **60** were less potent PqsD inhibitors.

Hence, monocyclic heteroaromatic residues were introduced. For all the thiophene and pyridine derivatives **61**, **62**, and **65–67** moderate activity without further improvement was observed. The furane derivatives showed conspicuous behaviour, since the differences in activity between the oxygen in 2- or 3-position were tremendous. While the 3-furyl derivative **64** was almost inactive, the 2-furyl isomer **63** shows improved PqsD inhibition. The synthetic route towards fluorescent (2-nitrophenyl)methanol derivatives provided additional inhibitors of PqsD with non-fluorescent residues R as intermediates. The amines **77–79** may be considered as direct derivatives of the alkyl compounds **49–51**, whereas the terminal methyl was substituted by an amino group, which is expected to be protonated under assay conditions. In contrast

Table 1 PqsD inhibition by (2-nitrophenyl)methanol derivatives

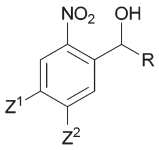

Compounds	Z^1	Z^2	R	IC_{50} [μM] (10 min)[a,b]	IC_{50} [μM] (30 min)[a,c]
3	H	H	Ph	3.2 ± 0.1	0.5 ± 0.1
33	Cl	H	Ph	13.4 ± 1.4	11.2 ± 0.9
34	H	Cl	Ph	15.0 ± 0.6	1.6 ± 0.1
35	NO_2	H	Ph	15.4 ± 2.0	5.8 ± 1.0
39	Me	H	Ph	3.7 ± 0.5	1.6 ± 0.1
40	H	Me	Ph	1.9 ± 0.4	0.6 ± 0.1
43	OMe	H	Ph	2.2 ± 0.5	1.6 ± 0.3
44	H	OMe	Ph	3.0 ± 0.4	0.5 ± 0.1
45	H	H	H	1.6 ± 0.5	0.7 ± 0.2
47	H	H	Me	1.3 ± 0.3	0.8 ± 0.1
48	H	H	Et	1.1 ± 0.2	0.8 ± 0.1
49	H	H	*n*-Pr	2.8 ± 0.4	1.0 ± 0.4
50	H	H	*n*-Bu	5.2 ± 0.8	2.9 ± 0.1
51	H	H	*n*-Pentyl	4.9 ± 0.9	1.0 ± 0.4
52	H	H	iso-Bu	7.9 ± 1.0	1.2 ± 0.3
53	H	H	*tert*-Pentyl	15.9 ± 1.1	6.7 ± 0.1
54	H	H	*c*-Pentyl	4.9 ± 1.0	1.4 ± 0.2
55	H	H	*c*-Hexyl	10.1 ± 1.4	4.5 ± 0.2
56	H	H	1-Adamantyl	11.6 ± 2.2	2.7 ± 0.1
57	H	H	CH_2Ph	5.4 ± 0.6	0.8 ± 0.1
58	H	H	CH_2CH_2Ph	4.6 ± 1.0	0.9 ± 0.1
59	H	H	1-Naphthyl	10.8 ± 2.5	5.8 ± 0.2
60	H	H	2-Naphthyl	13.1 ± 1.9	2.4 ± 0.5
61	H	H	2-Thienyl	14.3 ± 1.9	1.5 ± 0.2
62	H	H	3-Thienyl	5.9 ± 0.9	6.4 ± 1.9
63	H	H	2-Furyl	1.8 ± 0.4	0.9 ± 0.1
64	H	H	3-Furyl	28% @ 50 μM	13.1 ± 2.8
65	H	H	2-Pyridyl	6.7 ± 1.2	1.2 ± 0.1
66	H	H	3-Pyridyl	11.7 ± 2.1	1.7 ± 0.1
67	H	H	4-Pyridyl	6.8 ± 1.4	2.2 ± 0.1
68	H	H	$(CH_2)_2$Phth	1.2 ± 0.1	0.3 ± 0.1
69	H	H	$(CH_2)_3$Phth	1.9 ± 0.3	0.7 ± 0.2
70	H	H	$(CH_2)_4$Phth	1.7 ± 0.5	1.6 ± 0.4
71	H	Me	Et	0.7 ± 0.3	0.6 ± 0.1
72	H	Me	2-Thienyl	6.2 ± 1.8	2.7 ± 0.5
73	H	Me	3-Thienyl	3.3 ± 0.5	1.6 ± 0.3
74	H	Me	2-Furyl	0.9 ± 0.1	1.1 ± 0.1
75	H	Me	$(CH_2)_2$Phth	0.9 ± 0.1	0.7 ± 0.1
76	H	Me	$(CH_2)_3$Phth	0.7 ± 0.1	0.7 ± 0.2
77	H	H	$(CH_2)_2NH_2$	34.7 ± 4.6	40.0 ± 3.7
78	H	H	$(CH_2)_3NH_2$	44% @ 50 μM	27.8 ± 1.7
79	H	H	$(CH_2)_4NH_2$	8.2 ± 2.1	22.4 ± 4.3
80[d]				3.5 ± 0.1	5.8 ± 0.2
81[d]				3.0 ± 1.3	4.0 ± 0.7
82[d]				3.2 ± 0.4	1.4 ± 0.3
83[d]				4.3 ± 0.5	3.4 ± 0.2
84[d]				46.5 ± 2.1	12.5 ± 4.2
85[d]				13.1 ± 1.5	10.0 ± 0.7
86[d]				1.3 ± 0.7	1.5 ± 0.3

[a] *P. aeruginosa* PqsD (recombinantly expressed in *Escherichia coli*), anthraniloyl-CoA (5 μM), and β-ketodecanoic acid (70 μM). [b] IC_{50} values were determined using a 10 min preincubation period of inhibitor and enzyme followed by a 40 min reaction time. [c] IC_{50} values were determined using a 30 min preincubation period of inhibitor and enzyme followed by a 40 min reaction time. [d] For the structure of the fluorescent derivatives **80–86** see Scheme 2.

to the alkyl compounds, the amines **77–79** showed low activity. This result was expected, as the entrance of the substrate tunnel is decorated with arginine side chains providing a repulsive positive surface polarization.

The phthalimides **68–70**, on the other hand, also differing in the length of the alkyl linker, showed potent PqsD inhibition. Compound **68** even demonstrated the lowest IC_{50} value within the investigated set of compounds of around 300 nM.

So far, novel interesting derivatives with retained potency and reduced molecular weight (**45**, **47**, **48**, and **63**) or even improved target affinity (**68**) have been identified. Moreover, some compounds showed a pronounced difference between the IC_{50} values measured *via* the 10 min and 30 min protocol (**34**, **52**, **61**, and **66**) indicating a slow onset of inhibition. As described above, introduction of a methyl group in *para* position to the nitro group resulted in a reduction of time-dependency while retaining activity for compound **40**. These results encouraged us to synthesize additional selected derivatives possessing this methyl group (**71**, **72**). Indeed, all of these methyl-containing compounds showed a fast onset of inhibition (Table 1) while being potent inhibitors of PqsD in the single-digit micromolar to submicromolar range. However, no further improvement in target affinity has been gained compared to the most potent compound **68**. Nevertheless, together with the unmethylated congeners (**48**, **61–63**, **68**, and **69**) interesting pairs of PqsD inhibitors for further evaluation *in cellulo* have been yielded.

Apparently, various substituents of R are tolerated by PqsD, which encouraged us to introduce fluorescent groups in this position. Since promising inhibitory activity was observed for compound **2**, we substituted the pantothenate moiety by dansyl (5-(dimethylamino)-naphthalene-1-sulfonyl), NBD (7-nitrobenz-2-oxa-1,3-diazol-4-yl) and fluorescein fluorophores. The flexible linker of **2** was conserved to provide sufficient degrees of conformational freedom to adopt to the sterical requirements of the substrate tunnel. In the case of the dansyl derivatives **80–82**, the chain length of the alkyl linker was only slightly varied with the intention to position the hydrophobic fluorophore within the channel. For the more hydrophilic NBD derivatives **83–85** additional acyl linkers were introduced as well, thereby shifting the fluorophore towards the protein surface. Fortunately, an acceptable *in vitro* activity was observed for the dansyl derivatives **80–82**, and compounds with NBD (**83**) or fluorescein (**86**) directly attached to the amine **78**. However, the NBD fluorophores **84** and **85** containing an additional acyl-linker were less potent. Unfavourable interactions and/or entropic penalties might be possible reasons.

Table 2 Comparison of inhibitory potency regarding HHQ production in a *P. aeruginosa pqsH* mutant with physicochemical properties

Cmpd	MW[a]	Log P[a,b]	LE[a,c]	IC_{50} (10 min)/IC_{50} (30 min)[a]	% HHQ inhibition[d]
3	229.23	2.47	0.52	6.4	43 ± 6
33	263.68	3.16	0.39	1.2	n.i.
34	263.68	3.12	0.45	9.4	n.i.
35	274.23	2.14	0.37	2.7	10 ± 4
39	243.26	2.93	0.45	2.3	20 ± 3
40	243.26	2.93	0.48	3.2	19 ± 7
43	259.26	2.69	0.43	1.4	n.i.
44	259.26	2.55	0.46	6.0	n.i.
45	153.14	0.76	0.78	2.3	13 ± 1
47	167.16	1.11	0.71	1.6	26 ± 6
48	181.19	1.64	0.66	1.4	61 ± 2
49	195.22	2.17	0.60	2.8	22 ± 7
50	209.24	2.71	0.52	1.7	n.i.
51	223.27	3.24	0.53	4.9	n.i.
61	235.26	2.15	0.51	8.7	64 ± 6
62	235.26	2.15	0.45	0.8	74 ± 6
63	219.19	1.63	0.53	2.0	51 ± 15
64	219.19	1.63	0.43	n.d.[e]	73 ± 2
68	326.30	2.61	0.38	4.0	n.i. @ 125 μM
69	340.33	2.84	0.34	2.7	n.i. @ 125 μM
70	354.36	2.98	0.31	1.1	n.i. @ 125 μM
71	195.22	2.10	0.62	1.2	n.i.
72	249.24	2.61	0.46	2.3	24 ± 0.2
73	249.24	2.61	0.48	2.1	23 ± 7
74	233.22	2.09	0.49	0.8	20 ± 2
75	340.33	3.07	0.34	1.3	n.i. @ 125 μM
76	354.36	3.30	0.33	1.0	n.i. @ 100 μM
80	429.49	3.71	0.24	0.6	n.i. @ 75 μM
81	443.52	3.94	0.24	0.8	n.i. @ 75 μM
82	457.54	4.08	0.26	2.3	n.i. @ 25 μM
83	373.32	1.10	0.28	1.3	n.i. @ 150 μM
84	444.40	2.15	0.21	3.7	17 ± 3
85	486.48	2.65	0.20	1.3	27 ± 1
86	599.61	2.94	0.19	0.9	n.i.

[a] Molecular weight (MW), calculated partition coefficient (log P), ligand efficiency index (LE), and the ratio of IC_{50} values measured using different preincubation periods. [b] Calculated by ACD/Labs 2012 using the ACD/Log P Classic algorithm. [c] Values calculated as LE = 1.4 (−log IC_{50})/N using the IC_{50} value for the prolonged incubation time (30 min) and N meaning number of non-hydrogen atoms. [d] Planctonic *P. aeruginosa* PA14 *pqsH* mutant. Inhibitor concentration 250 μM as not indicated otherwise. Percentage of inhibition was normalized regarding OD600. n.i. no significant inhibition (<10%). [e] n.d. means "not determined".

Inhibition of signal molecule production in a *P. aeruginosa pqsH* mutant

In an attempt to elucidate the physicochemical and/or functional requirements for high *in cellulo* efficacy, we tested selected compounds regarding their ability to reduce the signal molecule levels in *P. aeruginosa* PA14 (Table 2).

In the wild-type strain, HHQ is converted into PQS by PqsH and the expression of *pqsH* depends on the growth period.[26] Thus, we quantified HHQ in a *pqsH* mutant, which is not able to perform this oxidation, to increase simplicity and reproducibility of this cell-based assay. To ensure the validity of this novel methodology, we compared the results gathered using the *pqsH* mutant with additionally determined PA14 wild-type data for three selected compounds and observed a good correlation between both data sets (see ESI†).

If soluble, all compounds were tested at 250 μM. The *in cellulo* results are summarized in Table 2 together with relevant parameters like molecular weight (MW), calculated partition coefficient (log P), ligand efficiency index (LE), and the ratio of IC_{50} values measured using different preincubation periods.

Inhibitor **3**, which served as a starting point, decreased HHQ production by 43%. Introduction of methyl groups into the nitro-phenyl moiety (**39** and **40**) reduced inhibitory potency, whereas methoxy substituents (**43** and **44**) led to inactivity. These results are disappointing, since two of the compounds showed submicromolar *in vitro* activity. A similar result was obtained for molecules bearing a substituent in the nitrophenyl moiety: the chloro compounds **33** and **34** as well as the dinitrophenyl-derivative **35** showed no or only low

activity in the cells. Furthermore, no effects on HHQ production despite of most promising IC_{50} values were observed for the phthalimides **68–70**, **75**, and **76**, which were tested at 100–125 μM due to limited solubility.

All congeners of the homologous series **45–51** containing unbranched alkyl residues showed good activity in the enzymatic assay, whereas the *in vitro* activity slightly decreased for the larger alkanes. In the cellular test system, the largest residues (**50** and **51**) led to inactivity, while a maximum HHQ inhibition was observed for ethyl (**48**). This compound showed an improved cellular activity compared to the starting point **3**. Interestingly, the variant with methyl in *para* position to the nitro group (**71**) was inactive, although it possesses a slightly improved IC_{50} value.

Surprisingly, all four compounds containing heteroaromatic pentacycles **61–64** potently reduced the HHQ formation. These compounds were not among the most potent PqsD inhibitors *in vitro*. Moreover, **64** showed only a moderate activity in the double-digit micromolar range against recombinant PqsD. We can only speculate whether additional alternative cellular targets are involved or whether the furanyl residue is converted into a more active compound inside the cell. Multiple examples for the instability of furan are reported in the literature. However, the thiophene **62** is the most potent inhibitor of cellular HHQ formation reported so far. Again, the methyl modification in Z^2 of the nitrophenyl moiety resulting in compounds **72–74** was detrimental to *in cellulo* efficacy.

Finally, we examined the effect of fluorophore-labelled derivatives **80–86** on *P. aeruginosa* to evaluate their potential for applications in cellular systems. Unfortunately, neither the dansyl- nor fluorescein-labelled inhibitors (**80–82** and **86**) were able to reduce HHQ formation at 250 μM. Consequently, their application is restricted to studies using lysed cells or isolated biomolecules. The best results were obtained for NBD derivatives **84** and **85**, which showed at least slight inhibition. This opens up avenues towards intracellular labelling experiments, which might be conducted in the future.

Interpretation of *in vitro* and *in cellulo* data

A first conclusion which can be drawn from the detailed experimental data reported herein is that in the case of (2-nitrophenyl)methanol derivatives *in vitro* potency expressed either as IC_{50} or ligand efficiency (LE, Table 2) does not directly translate into *in cellulo* activity. However, this observation is not utterly surprising as Gram-negative bacteria, in general, and *P. aeruginosa*, in particular, are known to provide challenging barriers for the effective inhibition of intracellular targets.[27–29] The orthogonal sieving ability of the two bacterial cell membranes blocking larger hydrophobic compounds (outer membrane) as well as smaller hydrophilic entities (inner membrane) from entering the cytoplasm is only one obstacle which an anti-infective agent has to overcome.[27,28] Additionally, an arsenal of efflux pumps and degrading/metabolizing enzymes may hinder a drug from reaching its target.[29] Hence, the physicochemical, structural, and functional features of compounds displaying intracellular activity are all the more worthwhile to investigate.

In this context, time-dependent inhibition was one characteristic of the presented compound class that has first drawn our attention. Reversible target interaction (inhibition) is characterized by inhibitor binding (k_{on}, "on-rate") and dissociation (k_{off}, "off-rate"). Thus, a slow binding behaviour in combination with promising (nanomolar) IC_{50} values would imply long drug-residence times as the "off-rate" should also be attenuated along with the inhibition onset ("on-rate"). Such an effective (long-lasting) enzyme blockade can be considered a favourable scenario in order to shut down cellular signal molecule synthesis. However, we were not able to establish a correlation between this phenomenon and improved HHQ reduction. Some compounds with either high or low ratios of IC_{50} values measured using 10 min or 30 min of preincubation were effective inhibitors of signal molecule production (compare for example **3** and **61** with **62** and **70**). Indeed, we showed that the methyl modification at the nitrophenyl core results in compounds with only low time-dependent onset of inhibition along with a decreased or even abolished *in cellulo* efficacy (**48** *vs.* **71** and **61** *vs.* **72**). Nevertheless, the most potent inhibitor in our cell assays was **62** showing almost no time-dependency of PqsD inhibition.

A parameter which seems to have direct influence on intracellular activity, though, was molecular weight. Most compounds with MW > 300 Da were inactive inside the cells. The only exceptions within the set of tested compounds were NBD-tagged fluorophores **84** and **85** showing only a moderate reduction of HHQ production. This observed mass cut-off is much lower than the general value of 600 Da reported for Gram-negative bacteria and should not be considered a strict criteria due exceptions mentioned above.[30] This finding might be explained by the described low permeability of outer membrane of *P. aeruginosa* compared to other Gram-negative bacteria.[31]

Another important physicochemical parameter for cellular availability is hydrophobicity usually expressed as the octanol–water partition coefficient log *P*. None of the fragment-like compounds reported herein can be considered as strongly lipophilic as none of them exceeds log $P \approx 4$ while the majority possesses a value below 3. However, it has been proposed by others that even lower log *P* values are beneficial or actually a prerequisite for activity against Gram-negative bacteria.[30] Indeed, our most active compound *in cellulo* possess a log *P* below 2.5.

Noteworthy, we have identified compounds within the set of tested (2-nitrophenyl)methanol derivatives that are interesting exceptions to the described MW/log *P* criteria. Compound **71**, for example, has low molecular weight (195.22 Da) and log *P* (0.62) combined with a substantial *in vitro* activity (IC_{50} = 0.6) but no relevant *in cellulo* activity. We account this finding to the general detrimental effect of the methyl group in *para* position to the nitro group which we have also found for the other compounds bearing this substitution pattern. On the other hand, developed NDB-tagged inhibitors possess

increased molecular weight and hydrophobicity, yet show moderate activity on signal molecule production. Hence, further optimization of our fragment-like molecules towards drug-like compounds *via* fragment growing approaches may be a rewarding endeavour.

Conclusions

More than fifty derivatives of (2-nitrophenyl)phenylmethanol **3** have been synthesized and tested for *in vitro* activity. In this regard, we demonstrated that 4-methoxyphenylmagnesium bromide is a suitable reagent to accomplish efficient I–Mg exchange for compound **42**. Whereas the nitro group in *ortho* position turned out to be essential for *in vitro* PqsD inhibition, no mutagenicity was observed for compound **3** in an Ames test. Improved potency was achieved by the replacement of the eastern phenyl residue. This position turned out to be very tolerant for various moieties, which allowed the design of fluorescence-labelled inhibitors.

For a straightforward evaluation of PqsD inhibitors in the cellular context, signal molecule production was investigated using a *pqsH*-deficient *P. aeruginosa* PA14 strain. Some of our compounds showed significantly improved inhibition of signal molecule production. An attempt to correlate *in vitro* data with *in cellulo* results has been made identifying low molecular weight and hydrophobicity as important, but not stringent, criteria for intracellular activity. Nevertheless, the presented work emphasizes the notion that optimization of intracellular activity is a challenging multi-parameter problem which requires further intense research.

Finally, novel PqsD inhibitors presented in this work possess a fragment-like size and improved efficiency *in cellulo*. Together with the structural insight provided by our studies regarding the mode of action, we have delivered the basis for a fragment-growing optimization process towards PqsD-targeting anti-infectives.

Experimental section

General

(2-Nitrophenyl)methanol **45** was purchased from Sigma-Aldrich and used for biological assays without further purification. Starting materials were purchased from ABCR, Acros, Sigma-Aldrich and Fluka and were used without further purification. All reactions were conducted under a nitrogen atmosphere. During workup drying was achieved by anhydrous sodium sulfate. Flash chromatography was performed using silica gel 60 (40–63 μm) and the reaction progress was determined by TLC analysis on ALUGRAM SIL G/UV254 (Macherey-Nagel). Visualization was accomplished through excitation using UV light. Purification by semi-preparative HPLC was carried out on an Agilent 1200 series HPLC system from Agilent Technologies, using an Agilent Prep-C18 column (30 × 100 mm/10 μm) as stationary phase with acetonitrile–water as eluent. The purity of compounds used in the biological assays was ≥95% as measured by LC/MS, monitored at 254 nm. The methods for LC/MS analysis and a table with analytical data (including melting points) for all tested compounds are provided in the purity section of the ESI.† All chiral alcohols were isolated as racemates. ^{1}H and ^{13}C NMR spectra were recorded on a Bruker DRX-500 instrument at 300 K. Chemical shifts are reported in δ values (ppm) and the hydrogenated residues of deuterated solvents were used as internal standard (acetone-d_6: 2.05, 29.84. $CDCl_3$: δ = 7.26, 77.16. MeOH-d_4: δ = 3.31, 49.00. DMSO-d_6: δ = 2.50, 39.52). Splitting patterns describe apparent multiplicities and are designated as s (singlet), d (doublet), dd (doublet of doublet), t (triplet), td (triplet of doublet), q (quartet), m (multiplet). All coupling constants (J) are given in hertz (Hz). Mass spectra (ESI) were measured on a Thermo Scientific Orbitrap. Mass spectra (EI) were measured on a DSQII instrument (ThermoFisher). Melting points of samples were determined in open capillaries using a SMP3 Melting Point Apparatus from Bibby Sterilin and are uncorrected. Infrared spectra were measured on a PerkinElmer Spectrum 100 FT-IR spectrometer.

General method A for synthesis of 3, 39, 40, 48–76

A solution of 2-iodo-nitrobenzene **36** or a close derivative (1.0 eq.) in THF (10 ml g^{-1} reagent) was cooled to −40 °C and a solution of phenylmagnesium chloride (2 M in THF, 1.1 eq.) was added dropwise. After stirring for 30 min at −40 °C, the aldehyde (1.0 eq.) was added. Then, the reaction mixture was continuously stirred at −40 °C until complete conversion (checked by TLC). The reaction was quenched with a saturated solution of NH_4Cl (5 ml) and diluted with water (5 ml). The aqueous phase was extracted with ethyl acetate (three times) and the combined organic layers were washed with brine, dried, and concentrated under reduced pressure. The residue was purified by column chromatography over silica gel to give the desired product.

General method B for synthesis of 10, 14, and 15

A solution of the iodobenzene **9**, **12** or **13** (1.00 g, 1.0 eq.) in 30 ml THF was cooled to −40 °C and a solution of iso-propylmagnesium chloride (2 M in THF, 1.1 eq.) was added dropwise. The solution was stirred for 60 min at −40 °C, benzaldehyde (1.0 eq.) was added and the reaction was completed at −40 °C (checked by TLC). The workup was carried out as described in method A.

General method C for synthesis of 21–25

To a solution of phenylmagnesium chloride (2 M in THF, 1.5 eq.) in 8 ml THF at 0 °C aldehydes **16–20** (1 eq.) were slowly added and the solution was stirred at 50 °C for 30 min. The mixture was cooled to 0 °C, quenched with a saturated solution of NH_4Cl (5 ml), and diluted with water (5 ml). The aqueous phase was extracted with diethyl ether (three times) and the combined organic layers were dried and concentrated under reduced pressure. The residue was purified by column chromatography over silica gel to give the desired product.

General method D for synthesis of 28 and 29

To a solution of phenylmagnesium chloride (3.31 ml, 2 M in THF, 6.62 mmol) in 20 ml THF at −40 °C nitrobenzaldehyde **26** or **27** (1.00 g, 6.62 mmol) was added slowly. The reaction mixture was stirred continuously at −40 °C until complete conversion (checked by TLC). The mixture was quenched with a saturated solution of NH_4Cl (5 ml) and diluted with water (5 ml). The workup was carried out as described in method A, followed by purification of the crude product by flash chromatography (petroleum ether–ethyl acetate 6 : 1).

General method E for synthesis of 77–79

To a solution of the phthalimides **68–70** (1.53 mmol, 1 eq.) in ethanol (40 ml) hydrazine hydrate (9.18 mmol, 6 eq.) was added and the mixture was refluxed for 3 h. Ethanol was removed *in vacuo* and ethyl acetate was added. The solution was washed with water and extracted twice with EtOAc. The organic phase was dried and the solvent was evaporated to yield the desired product in sufficient purity.

Expression and purification of recombinant PqsD

Expression and purification of recombinant PqsD was conducted as previously described.[16] Briefly, BL21 (λDE3) *E. coli* transformed with expression vector pT28b(+)/*pqsD* were induced with IPTG overnight. After harvesting and lysis through sonication, recombinant PqsD possessing a His_6-tag was isolated *via* immobilized metal ion affinity chromatography (IMAC) followed by gel filtration. The affinity tag was removed by thrombin cleavage and a second IMAC step.

Enzyme inhibition assay using recombinant PqsD

The standard assay for determination of IC_{50} values was performed monitoring the enzyme activity by measuring the HHQ concentration as described recently.[14] PqsD was preincubated with inhibitor for 10 min or 30 min prior to addition of the substrates ACoA and β-ketodecanoic acid. Quantification of HHQ was performed analogously, but with some modifications: The flow rate was set to 750 µl min^{-1} and an Accucore RP-MS column, 150 × 2.1 mm, 2.6 µm, (Thermo Scientific) was used. All test compound reactions were performed in sextuplicate. Synthesis of ACoA and β-ketodecanoic acid was performed as described in the ESI.†

Cultivation of *P. aeruginosa* PA14 *pqsH* mutant

For determination of extracellular HHQ levels, cultivation was performed in the following way: cultures of *P. aeruginosa* PA14 *pqsH* transposon mutant[23] (initial OD_{600} = 0.02) were incubated with or without inhibitor (final DMSO concentration 1%, v/v) at 37 °C, 200 rpm and a humidity of 75% for 16 h in 24-well Greiner Bio-One Cellstar plates (Frickenhausen, Germany) containing 1.5 ml medium per well. Cultures were generally grown in PPGAS medium (20 mM NH_4Cl, 20 mM KCl, 120 mM Tris-HCl, 1.6 mM $MgSO_4$, 0.5% (w/v) glucose, 1% (w/v) Bacto™ Tryptone). For each sample, cultivation and sample work-up were performed in triplicates.

Determination of extracellular HHQ levels

Extracellular levels of HHQ were determined according to the method of Lépine *et al.* with the following modifications.[32,33] An aliquot of 500 µl of bacterial cultures were supplemented with 50 µl of a 10 µM methanolic solution of the internal standard (IS) 5,6,7,8-tetradeutero-2-heptyl-4(1*H*)-quinolone (HHQ-d_4) and extracted with 1 ml of ethyl acetate by vigorous shaking. After centrifugation, 400 µl of the organic phase were evaporated to dryness in LC glass vials. The residue was re-dissolved in methanol. UHPLC-MS/MS analysis was performed as described in detail recently.[16] The following ions were monitored (mother ion [*m*/*z*], product ion [*m*/*z*], scan time [s], scan width [*m*/*z*], collision energy [V], tube lens offset [V]): HHQ: 244, 159, 0.5, 0.01, 30, 106; HHQ-d_4 (IS): 248, 163, 0.1, 0.01, 32, 113. Xcalibur software was used for data acquisition and quantification with the use of a calibration curve relative to the area of the IS.

Calculation of log *P* values

Experimental values of **67** and **79** were determined by Sirius T3 titrator from Sirius Analytical. Comparison with values calculated by ACD/Labs 2012 (Build 1996, 31. May 2012) revealed, that ACD/Log *P* Classic is the most appropriate algorithm. Consequently, the latter was used for the values given in Table 2.

Abbreviations

2-ABA	2-Aminobenzoylacetate
ACoA	Anthraniloyl-CoA
dansyl	5-(Dimethylamino)-naphthalene-1-sulfonyl
EDG/EWG	Electron-donating/withdrawing group
HHQ	2-Heptyl-4-quinolone
LE	Ligand efficiency
log *P*	Octanol–water partition coefficient
MW	Molecular weight
NBD	7-Nitrobenz-2-oxa-1,3-diazol-4-yl
PQS	2-Heptyl-3-hydroxy-4-quinolone
QS	*Quorum sensing*

Acknowledgements

We thank Carina Scheid, Simone Amann, and Christine Maurer for performing the PqsD and cellular assays. Furthermore, we thank Prof. Dr Susanne Häußler for kindly supplying the *P. aeruginosa* PA14 wild-type strain and PA14 *pqsH* mutant and Michael Hoffmann for performing HRMS measurements.

Notes and references

1 S. Swift, J. A. Downie, N. A. Whitehead, A. M. Barnard, G. P. Salmond and P. Williams, *Adv. Microb. Physiol.*, 2001, **45**, 199.

2 For a review see: L. C. M. Antunes, R. B. R. Ferreira, M. M. C. Buckner and B. B. Finlay, *Microbiology*, 2010, **156**, 2271.
3 L. Yang, M. Nilsson, M. Gjermansen, M. Givskov and T. Tolker-Nielsen, *Mol. Microbiol.*, 2009, **74**, 1380.
4 T. B. Rasmussen and M. Givskov, *Microbiology*, 2006, **152**, 895.
5 J. C. A. Janssens, S. C. J. De Keersmaecker, D. E. De Vos and J. Vanderleyden, *Curr. Med. Chem.*, 2008, **15**, 2144.
6 For a critical discussion see: T. Defoirdt, N. Boon and P. Bossier, *PLoS Pathog.*, 2010, **6**, e1000989.
7 E. C. Pesci, J. B. Milbank, J. P. Pearson, S. L. McKnight, A. Kende, E. P. Greenberg and B. Iglewski, *Proc. Natl. Acad. Sci. U. S. A.*, 1999, **96**, 11229.
8 J.-F. Dubern and S. P. Diggle, *Mol. BioSyst.*, 2008, **4**, 882.
9 C. Lu, B. Kirsch, C. Zimmer, J. C. de Jong, C. Henn, C. K. Maurer, M. Müsken, S. Häussler, A. Steinbach and R. W. Hartmann, *Chem. Biol.*, 2011, **19**, 381.
10 C. Lu, C. K. Maurer, B. Kirsch, A. Steinbach and R. W. Hartmann, *Angew. Chem., Int. Ed.*, 2014, **53**, 1109.
11 L. A. Gallagher, S. L. McKnight, M. S. Kuznetsowa, E. C. Pesci and C. Manoil, *J. Bacteriol.*, 2002, **184**, 6472.
12 Y.-M. Zhang, M. W. Frank, K. Zhu, A. Mayasundari and C. O. Rock, *J. Biol. Chem.*, 2008, **283**, 28788.
13 C. E. Dulcey, V. Dekimpe, D.-A. Fauvelle, S. Milot, M.-C. Groleau, N. Doucet, L. G. Rahme, F. Lépine and E. Déziel, *Chem. Biol.*, 2013, **20**, 1481.
14 D. Pistorius, A. Ullrich, S. Lucas, R. W. Hartmann, U. Kazmaier and R. Müller, *ChemBioChem*, 2011, **12**, 850.
15 E. Weidel, J. C. de Jong, C. Brengel, M. P. Storz, A. Braunshausen, M. Negri, A. Plaza, A. Steinbach, R. Müller and R. W. Hartmann, *J. Med. Chem.*, 2013, **56**, 6146.
16 M. P. Storz, C. K. Maurer, C. Zimmer, N. Wagner, C. Brengel, J. C. de Jong, S. Lucas, M. Müsken, S. Häussler, A. Steinbach and R. W. Hartmann, *J. Am. Chem. Soc.*, 2012, **134**, 16143.
17 M. P. Storz, C. Brengel, E. Weidel, M. Hoffmann, K. Hollemeyer, A. Steinbach, R. Müller, M. Empting and R. W. Hartmann, *ACS Chem. Biol.*, 2013, **8**, 2794.
18 J. H. Sahner, C. Brengel, M. P. Storz, M. Groh, A. Plaza, R. Müller and R. W. Hartmann, *J. Med. Chem.*, 2013, **56**, 8656.
19 B. Lesic, F. Lépine, E. Déziel, J. Zhang, Q. Zhang, K. Padfield, M.-H. Castonguay, S. Milot, S. Stachel, A. A. Tzika, R. G. Tompkins and L. G. Rahme, *PLoS Pathog.*, 2007, **3**, e126.
20 R. Padda, C. Wang, J. Hughes, R. Kutty and G. Bennett, *Environ. Toxicol. Chem.*, 2003, **22**, 2293.
21 S. Xu, A. N. Butkevich, R. Yamada, Y. Zhou, B. Debnath, R. Duncan, E. Zandi, N. A. Petasis and N. Neamati, *Proc. Natl. Acad. Sci. U. S. A.*, 2012, **109**, 16348.
22 K. A. Kozlowski, F. H. Wezeman and R. M. Schultz, *Proc. Natl. Acad. Sci. U. S. A.*, 1984, **81**, 1135.
23 N. T. Liberati, J. M. Urbach, S. Miyata, D. G. Lee, E. Drenkard, G. Wu, J. Villanueva, T. Wei and F. M. Ausubel, *Proc. Natl. Acad. Sci. U. S. A.*, 2006, **103**, 2833.
24 I. Sapountzis and P. Knochel, *Angew. Chem., Int. Ed.*, 2002, **41**, 1610.
25 R. A. Copeland, D. L. Pompliano and T. D. Meek, *Nat. Rev. Drug Discovery*, 2006, **5**, 730.
26 E. Déziel, F. Lépine, S. Milot, J. He, M. N. Mindrinos, R. Tompkins and L. G. Rahme, *Proc. Natl. Acad. Sci. U. S. A.*, 2004, **101**, 1345.
27 L. L. Silver, *Clin. Microbiol. Rev.*, 2011, **24**, 71.
28 H. Nikaido, *Antimicrob. Agents Chemother.*, 1989, **33**, 1831.
29 K. Poole, *J. Mol. Microbiol. Biotechnol.*, 2001, **3**, 255.
30 R. O'Shea and H. E. Moser, *J. Med. Chem.*, 2008, **51**, 2871.
31 B. L. Angus, A. M. Carey, D. A. Caron, A. M. Kropinski and R. E. Hancock, *Antimicrob. Agents Chemother.*, 1982, **21**, 299.
32 C. K. Maurer, A. Steinbach and R. W. Hartmann, *J. Pharm. Biomed. Anal.*, 2013, **86**, 127.
33 F. Lépine, F. E. Déziel, S. Milot and L. G. Rahme, *Biochim. Biophys. Acta*, 2003, **1622**, 36.

